



HAL
open science

Analysis and calibration of a linear model for structured cell populations with unidirectional motion : Application to the morphogenesis of ovarian follicles

Frédérique Clément, Frédérique Robin, Romain Yvinec

► To cite this version:

Frédérique Clément, Frédérique Robin, Romain Yvinec. Analysis and calibration of a linear model for structured cell populations with unidirectional motion : Application to the morphogenesis of ovarian follicles. 2018. hal-01852560v1

HAL Id: hal-01852560

<https://hal.science/hal-01852560v1>

Preprint submitted on 1 Aug 2018 (v1), last revised 7 Mar 2019 (v2)

HAL is a multi-disciplinary open access archive for the deposit and dissemination of scientific research documents, whether they are published or not. The documents may come from teaching and research institutions in France or abroad, or from public or private research centers.

L'archive ouverte pluridisciplinaire **HAL**, est destinée au dépôt et à la diffusion de documents scientifiques de niveau recherche, publiés ou non, émanant des établissements d'enseignement et de recherche français ou étrangers, des laboratoires publics ou privés.

1 **ANALYSIS AND CALIBRATION OF A LINEAR MODEL FOR**
2 **STRUCTURED CELL POPULATIONS WITH UNIDIRECTIONAL**
3 **MOTION : APPLICATION TO THE MORPHOGENESIS OF**
4 **OVARIAN FOLLICLES***

5 FRÉDÉRIQUE CLÉMENT [†], FRÉDÉRIQUE ROBIN [‡], AND ROMAIN YVINEC [§]

6 **Abstract.** We analyze a multi-type age dependent model for cell populations subject to uni-
7 directional motion, in both a stochastic and deterministic framework. Cells are distributed into
8 successive layers; they may divide and move irreversibly from one layer to the next. We adapt re-
9 sults on the large-time convergence of PDE systems and branching processes to our context, where
10 the Perron-Frobenius or Krein-Rutman theorem can not be applied. We derive explicit analytical
11 formulas for the asymptotic cell number moments, and the stable age distribution. We illustrate
12 these results numerically and we apply them to the study of the morphodynamics of ovarian folli-
13 cles. We prove the structural parameter identifiability of our model in the case of age independent
14 division rates. Using a set of experimental biological data, we estimate the model parameters to fit
15 the changes in the cell numbers in each layer during the early stages of follicle development.

16 **Key words.** structured cell populations, multi-type age dependent branching processes, renewal
17 equations, McKendrick-VonFoerster model, parameter calibration, structural identifiability

18 **AMS subject classifications.** 35L65, 60K15, 60J80, 92D25

19 **1. Introduction.** We study a multi-type age dependent model in both a de-
20 terministic and stochastic framework to represent the dynamics of a population of
21 cells distributed into successive layers. The model is a two dimensional structured
22 model: cells are described by a continuous age variable and a discrete layer index
23 variable. Cells may divide and move irreversibly from one layer to the next. The cell
24 division rate is age and layer dependent, and is assumed to be bounded below and
25 above. After division, the age is reset and the daughter cells either remain within
26 the same layer or move to the next one. In its stochastic formulation, our model is a
27 multi-type Bellman-Harris branching process and in its deterministic formulation, it
28 is a multi-type McKendrick-VonFoerster system.

29 The model enters the general class of linear models leading to Malthusian expo-
30 nential growth of the population. In the PDE case, state-of-the-art-methods call to
31 renewal equations system [6] or, to an eigenvalue problem and general relative entropy
32 techniques [7, 9] to show the existence of an attractive stable age distribution. Yet,
33 in our case, the unidirectional motion prevents us from applying the Krein-Rutman
34 theorem to solve the eigenvalue problem. As a consequence, we follow a constructive
35 approach and explicitly solve the eigenvalue problem. On the other hand, we adapt
36 entropy methods using weak convergences in \mathbf{L}^1 to obtain the large-time behavior
37 and lower bound estimates of the speed of convergence towards the stable age dis-
38 tribution. In the probabilistic case, classical methods rely on renewal equations [2]
39 and martingale convergences [3]. Using the same eigenvalue problem as in the deter-
40 ministic study, we derive a martingale convergence giving insight into the large-time
41 fluctuations around the stable state. Again, due to the lack of reversibility in our
42 model, we cannot apply the Perron-Frobenius theorem to study the asymptotic of
43 the renewal equations. Nevertheless, we manage to derive explicitly the stationary

*Submitted to the editors DATE.

[†]Project team MYCENAE, Centre INRIA de Paris, France. (frederique.clement@inria.fr).

[‡]Project team MYCENAE, Centre INRIA de Paris, France. (frederique.robin@inria.fr).

[§]PRC, INRA, CNRS, IFCE, Université de Tours, 37380 Nouzilly, France. (romain.yvinec@inra.fr).

44 solution of the renewal equations for the cell number moments in each layer as in [2].
 45 We recover the deterministic stable age distribution as the solution of the renewal
 46 equation for the mean age distribution.

47 The theoretical analysis of our model highlights the role of one particular layer:
 48 the leading layer characterized by a maximal intrinsic growth rate which turns out
 49 to be the Malthus parameter of the total population. The notion of a leading layer
 50 is a tool to understand qualitatively the asymptotic cell dynamics, which appears to
 51 operate in a multi-scale regime. All the layers upstream the leading one may extinct
 52 or grow with a rate strictly inferior to the Malthus parameter, while the remaining,
 53 downstream ones are driven by the leading layer.

54 We then check and illustrate numerically our theoretical results. In the stochastic
 55 case, we use a standard implementation of an exact Stochastic Simulation Algorithm.
 56 In the deterministic case, we design and implement a dedicated finite volume scheme
 57 adapted to the non-conservative form and dealing with proper boundary conditions.
 58 We verify that both the deterministic and stochastic simulated distributions agree
 59 with the analytical stable age distribution. Moreover, the availability of analytical
 60 formulas helps us to study the influence of the parameters on the asymptotic propor-
 61 tion of cells, Malthus parameter and stable age distribution.

62 Finally, we consider the specific application of ovarian follicle development in-
 63 spired by the model introduced in [1] and representing the proliferation of somatic
 64 cells and their organization in concentric layers around the germ cell. While the orig-
 65 inal model is formulated with a nonlinear individual-based stochastic formalism, we
 66 design a linear version based on branching processes and endowed with a straightfor-
 67 ward deterministic counterpart. We prove the structural parameter identifiability in
 68 the case of age independent division rates. Using a set of experimental biological data,
 69 we estimate the model parameters to fit the changes in the cell numbers in each layer
 70 during the early stages of follicle development. The main interest of our approach is
 71 to benefit from the explicit formulas derived in this paper to get insight on the regime
 72 followed by the observed cell population growth.

73 Beyond the ovarian follicle development, linear models for structured cell popu-
 74 lations with unidirectional motion may have several applications in life science mod-
 75 eling, as many processes of cellular differentiation and/or developmental biology are
 76 associated with a spatially oriented development (e.g. neurogenesis on the cortex, in-
 77 testinal crypt) or commitment to a cell lineage or fate (e.g. hematopoiesis, acquisition
 78 of resistance in bacterial strains).

79 The paper is organized as follows. In section 2, we describe the stochastic and
 80 deterministic model formulations and enunciate the main results. In section 3, we
 81 give the main proofs accompanied by numerical illustrations. Section 4 is dedicated
 82 to the application to the development of ovarian follicles. We conclude in section 5.
 83 Technical details and classical results are provided in Supplementary materials.

84 2. Model description and main results.

85 **2.1. Model description.** We consider a population of cells structured by age
 86 $a \in \mathbb{R}_+$ and distributed into layers indexed from $j = 1$ to $j = J \in \mathbb{N}^*$. The cells un-
 87 dergo mitosis after a layer-dependent stochastic random time $\tau = \tau^j$, ruled by an age-
 88 and-layer-dependent instantaneous division rate $b = b_j(a) : \mathbb{P}[\tau^j > t] = e^{-\int_0^t b_j(a) da}$.
 89 Each cell division time is independent from the other ones. At division, the age
 90 is reset and the two daughter cells may pass to the next layer according to layer-
 91 dependent probabilities. We note $p_{2,0}^{(j)}$ the probability that both daughter cells remain

92 on the same layer, $p_{1,1}^{(j)}$ and $p_{0,2}^{(j)}$, the probability that a single or both daughter cell(s)
 93 move(s) from layer j to layer $j + 1$, with $p_{2,0}^{(j)} + p_{1,1}^{(j)} + p_{0,2}^{(j)} = 1$. Note that the last
 layer is absorbing: $p_{2,0}^{(J)} = 1$. The dynamics of the model is summarized in Figure 1.

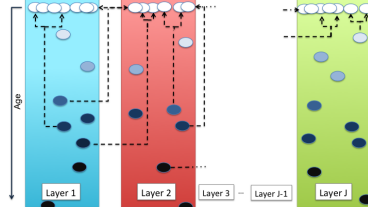


FIGURE 1. **Model description.** Each cell ages until an age-dependent random division time τ^j . At division time, the age is reset and the two daughter cells may move only in an unidirectional way. When $j = J$, the daughter cells stay on the last layer.

94

Stochastic model. Each cell in layer j of age a is represented by a Dirac mass $\delta_{j,a}$ where $(j, a) \in \mathcal{E} = \llbracket 1, J \rrbracket \times \mathbb{R}^+$. Let \mathcal{M}_P be the set of point measures on \mathcal{E} :

$$\mathcal{M}_P := \left\{ \sum_{k=1}^N \delta_{j_k, a_k}, N \in \mathbb{N}^*, \forall k \in \llbracket 1, N \rrbracket, (j_k, a_k) \in \mathcal{E} \right\}.$$

95 The cell population is represented for each time $t \geq 0$ by a measure $Z_t \in \mathcal{M}_P$:

$$96 \quad (1) \quad Z_t = \sum_{k=1}^{N_t} \delta_{I_t^{(k)}, A_t^{(k)}}, \quad N_t := \ll Z_t, \mathbf{1} \gg = \sum_{j=1}^J \int_0^{+\infty} Z_t(dj, da).$$

97 N_t is the total number of cells at time t . On the probability space $(\Omega, \mathcal{F}, \mathbb{P})$, we
 98 define Q as a Poisson point measure of intensity $ds \otimes \#dk \otimes d\theta$, where ds and $d\theta$ are
 99 Lebesgue measures on \mathbb{R}_+ and $\#dk$ is a counting measure on $\llbracket 1, J \rrbracket$. The dynamics
 100 of $Z = (Z_t)_{t \geq 0}$ is given by the following stochastic differential equation:

$$101 \quad (2) \quad Z_t = \sum_{k=1}^{N_0} \delta_{I_0^{(k)}, A_0^{(k)} + t} + \int_{[0, t] \times \mathcal{E}} \mathbf{1}_{k \leq N_{s-}} R(k, s, Z, \theta) Q(ds, dk, d\theta)$$

where $R(k, s, Z, \theta) = (2\delta_{I_{s-}^{(k)}, t-s} - \delta_{I_{s-}^{(k)}, A_{s-}^{(k)} + t-s}) \mathbf{1}_{0 \leq \theta \leq m_1(s, k, Z)}$
 $+ (\delta_{I_{s-}^{(k)}, t-s} + \delta_{I_{s-}^{(k)}+1, t-s} - \delta_{I_{s-}^{(k)}, A_{s-}^{(k)} + t-s}) \mathbf{1}_{m_1(s, k, Z) \leq \theta \leq m_2(s, k, Z)}$
 $+ (2\delta_{I_{s-}^{(k)}+1, t-s} - \delta_{I_{s-}^{(k)}, A_{s-}^{(k)} + t-s}) \mathbf{1}_{m_2(s, k, Z) \leq \theta \leq m_3(s, k, Z)}$

and $m_1(s, k, Z) = b_{I_{s-}^{(k)}}(A_{s-}^{(k)}) p_{2,0}^{(I_{s-}^{(k)})}$,
 $m_2(s, k, Z) = b_{I_{s-}^{(k)}}(A_{s-}^{(k)}) (p_{2,0}^{(I_{s-}^{(k)})} + p_{1,1}^{(I_{s-}^{(k)})})$, $m_3(s, k, Z) = b_{I_{s-}^{(k)}}(A_{s-}^{(k)})$.

102 *Deterministic model.* The cell population is represented by a population density
 103 function $\rho := (\rho^{(j)}(t, a))_{j \in \llbracket 1, J \rrbracket} \in \mathbf{L}^1(\mathbb{R}_+)^J$ where $\rho^{(j)}(t, a)$ is the cell age density in
 104 layer j at time t . The population evolves according to the following system of partial
 105 differential equations:

$$106 \quad (3) \quad \begin{cases} \partial_t \rho^{(j)}(t, a) + \partial_a \rho^{(j)}(t, a) = -b_j(a) \rho^{(j)}(t, a) \\ \rho^{(j)}(t, 0) = 2p_L^{(j-1)} \int_0^\infty b_{j-1}(a) \rho^{(j-1)}(t, a) da + 2p_S^{(j)} \int_0^\infty b_j(a) \rho^{(j)}(t, a) da \\ \rho(0, a) = \rho_0(a) \end{cases}$$

107 where $\forall j \in \llbracket 1, J-1 \rrbracket$, $p_S^{(j)} = \frac{1}{2}p_{1,1}^{(j)} + p_{2,0}^{(j)}$, $p_L^{(j)} := \frac{1}{2}p_{1,1}^{(j)} + p_{0,2}^{(j)}$, $p_L^{(0)} = 0$ and $p_S^{(J)} = 1$.

108 Here, $p_S^{(j)}$ is the probability that a cell taken randomly among both daughter cells,
109 remains on the same layer and $p_L^{(j)} = 1 - p_S^{(j)}$ is the probability that the cell moves.

110 2.2. Hypotheses.

111 *Hypothesis 2.1.* $\forall j \in \llbracket 1, J-1 \rrbracket$, $p_S^{(j)}, p_L^{(j)} \in (0, 1)$

112 *Hypothesis 2.2.* For each layer j , b_j is continuous bounded below and above:

$$113 \quad \forall j \in \llbracket 1, J \rrbracket, \quad \forall a \in \mathbb{R}_+, \quad 0 < b_j \leq b_j(a) \leq \bar{b}_j < \infty.$$

114 **DEFINITION 2.3.** \mathcal{B}_j is the distribution function of τ^j ($\mathcal{B}_j(x) = 1 - e^{-\int_0^x b_j(a) da}$)
115 and $d\mathcal{B}_j$ its density function ($d\mathcal{B}_j(x) = b_j(x)e^{-\int_0^x b_j(a) da}$).

116 *Hypothesis/Definition 2.4.* (Intrinsic growth rate) The intrinsic growth rate λ_j of
117 layer j is the solution of

$$118 \quad d\mathcal{B}_j^*(\lambda_j) := \int_0^\infty e^{-\lambda_j s} d\mathcal{B}_j(s) ds = \frac{1}{2p_S^{(j)}}.$$

119 *Remark 2.5.* $d\mathcal{B}_j^*$ is the Laplace transform of $d\mathcal{B}_j$. It is a strictly decreasing func-
120 tion and $]-b_j, \infty[\subset \text{Supp}(d\mathcal{B}_j^*) \subset]-\bar{b}_j, \infty[$. Hence, $\lambda_j > -\bar{b}_j$. Moreover, note that
121 $d\mathcal{B}_j^*(0) = \int_0^\infty d\mathcal{B}_j(x) dx = 1$. Thus, $\lambda_j < 0$ when $p_S^{(j)} < \frac{1}{2}$; $\lambda_j > 0$ when $p_S^{(j)} > \frac{1}{2}$ and
122 $\lambda_j = 0$ when $p_S^{(j)} = \frac{1}{2}$. In particular, $\lambda_J > 0$ as $p_S^{(J)} = 1$.

123 *Remark 2.6.* In the classical McKendrick-VonFoerster model (one layer), the
124 population grows exponentially with rate λ_1 ([16], Chap. IV). The same result is
125 shown for the Bellman-Harris process in [2] (Chap. VI).

126 *Hypothesis/Definition 2.7* (Malthus parameter). The Malthus parameter λ_c is
127 defined as the unique maximal element taken among the intrinsic growth rates (λ_j ,
128 $j \in \llbracket 1, J \rrbracket$) defined in (2.4). The layer such that the index $j = c$ is the leading layer.

129 According to remark 2.5, λ_c is positive. We will need auxiliary hypotheses on λ_j
130 parameters in some theorems.

131 *Hypothesis 2.8.* All the intrinsic growth rate parameters are distinct.

132 *Hypothesis 2.9.* $\forall j \in \llbracket 1, J \rrbracket$, $\lambda_j > -\liminf_{a \rightarrow +\infty} b_j(a)$.

133 Hypothesis 2.9 implies additional regularity for $t \mapsto e^{-\lambda_j t} d\mathcal{B}_j(t)$ (see proof in SM1.1):

134 **COROLLARY 2.10.** Under hypotheses 2.2, 2.4 and 2.9, $\forall j \in \llbracket 1, J \rrbracket$, $\forall k \in \mathbb{N}$,
135 $\int_0^\infty t^k e^{-\lambda_j t} d\mathcal{B}_j(t) dt < \infty$.

136 *Stochastic initial condition.* We suppose that the initial measure $Z_0 \in \mathcal{M}_P$ is
137 deterministic. $(\mathcal{F}_t)_{t \in \mathbb{R}_+}$ is the natural filtration associated with $(Z_t)_{t \in \mathbb{R}_+}$ and Q .

138 *Deterministic initial condition.* We suppose that the initial population density ρ_0
139 belongs to $\mathbf{L}^1(\mathbb{R}_+)^J$.

140 **2.3. Notation.** Let $f, g \in \mathbf{L}^1(\mathbb{R}_+)^J$, we use for the scalar product:

- 141 • on \mathbb{R}_+^J , $f^T(a)g(a) = \sum_{j=1}^J f^{(j)}(a)g^{(j)}(a)$,
- 142 • on $\mathbf{L}^1(\mathbb{R}_+)$, $\langle f^{(j)}, g^{(j)} \rangle = \int_0^\infty f^{(j)}(a)g^{(j)}(a) da$, for $j \in \llbracket 1, J \rrbracket$,
- 143 • on $\mathbf{L}^1(\mathbb{R}_+)^J$, $\ll f, g \gg = \sum_{j=1}^J \int_0^\infty f^{(j)}(a)g^{(j)}(a) da$.

144 For a martingale $M = (M_t)_{t \geq 0}$, we note $\langle M, M \rangle_t$ its quadratic variation. We also
 145 introduce

$$146 \quad B(a) = \text{diag}(b_1(a), \dots, b_J(a)), \quad [K(a)]_{i,j} = \begin{cases} 2p_S^{(j)} b_j(a), & i = j, \quad j \in \llbracket 1, J \rrbracket \\ 2p_L^{(j-1)} b_{j-1}(a), & i = j - 1, \quad j \in \llbracket 2, J \rrbracket \end{cases}$$

147 We define the primal problem (P) as

$$148 \quad (\text{P}) \quad \begin{cases} \mathcal{L}^P \hat{\rho}(a) = \lambda \hat{\rho}(a), \quad a \geq 0 \\ \hat{\rho}(0) = \int_0^\infty K(a) \hat{\rho}(a) da, \quad \mathcal{L}^P \hat{\rho}(a) = \partial_a \hat{\rho}(a) - B(a) \hat{\rho}(a), \\ \ll \hat{\rho}, \mathbf{1} \gg = 1 \text{ and } \hat{\rho} \geq 0 \end{cases}$$

149 and the dual problem (D) is given by

$$150 \quad (\text{D}) \quad \begin{cases} \mathcal{L}^D \phi(a) = \lambda \phi(a), \quad a \in \mathbb{R}_+^* \\ \ll \hat{\rho}, \phi \gg = 1 \text{ and } \phi \geq 0 \end{cases}, \quad \mathcal{L}^D \phi(a) = \partial_a \phi(a) - B(a) \phi + K(a)^T \phi(0).$$

151 2.4. Main results.

152 2.4.1. Eigenproblem approach.

153 **THEOREM 2.11** (Eigenproblem). *Under hypotheses 2.1, 2.2, 2.4, 2.7 and 2.9,*
 154 *there exists a first eigenelement triple $(\lambda, \hat{\rho}, \phi)$ solution to equations (P) and (D)*
 155 *where $\hat{\rho} \in \mathbf{L}^1(\mathbb{R}_+)^J$ and $\phi \in \mathcal{C}_b(\mathbb{R}_+)^J$. In particular, λ is the Malthus parameter λ_c*
 156 *given in Definition 2.7, and $\hat{\rho}$ and ϕ are unique.*

157 Beside the dual test function ϕ , we introduce other test functions to prove large-time
 158 convergence. Let $\hat{\phi}^{(j)}$, $j \in \llbracket 1, J \rrbracket$ be a solution of

$$159 \quad (4) \quad \partial_a \hat{\phi}^{(j)}(a) - (\lambda_j + b_j(a)) \hat{\phi}^{(j)}(a) = -2p_S^{(j)} b_j(a) \hat{\phi}^{(j)}(0), \quad \hat{\phi}^{(j)}(0) \in \mathbb{R}_+^*.$$

160 **THEOREM 2.12.** *Under hypotheses 2.1, 2.2, 2.4, 2.7 and 2.9, there exist polyno-*
 161 *mials $(\beta_k^{(j)})_{1 \leq k \leq j \leq J}$ of degree at most $j - k$ such that*

$$162 \quad (5) \quad \left\langle |e^{-\lambda_c t} \rho^{(j)}(t, \cdot) - \eta \hat{\rho}^{(j)}|, \hat{\phi}^{(j)} \right\rangle \leq \sum_{k=1}^j e^{-\mu_j t} \beta_k^{(j)}(t) \left\langle |\rho_0^{(k)} - \eta \hat{\rho}^{(k)}|, \hat{\phi}^{(k)} \right\rangle,$$

163 where $\eta := \ll \rho_0, \phi \gg$, $\mu_j := \lambda_c - \lambda_j > 0$ when $j \in \llbracket 1, J \rrbracket \setminus \{c\}$ and $\mu_c := \underline{b}_c$. In
 164 particular, there exist a polynomial β of degree at most $J - 1$ and constant μ such that

$$165 \quad \ll |e^{-\lambda_c t} \rho(t, \cdot) - \eta \hat{\rho}|, \hat{\phi} \gg \leq \beta(t) e^{-\mu t} \ll |\rho_0 - \eta \hat{\rho}|, \hat{\phi} \gg.$$

166 Using martingale techniques [3], we also prove a result of convergence for the stochastic
 167 process Z with the dual test function ϕ .

168 **THEOREM 2.13.** *Under hypotheses 2.1, 2.2, 2.4 and 2.7, $W_t^\phi = e^{-\lambda_c t} \ll \phi, Z_t \gg$*
 169 *is a square integrable martingale that converges almost surely and in \mathbf{L}^2 to a non-de-*
 170 *generate random variable W_∞^ϕ .*

171 **2.4.2. Renewal equation approach.** Using generating function methods de-
 172 veloped for multi-type age dependent branching processes (see [2], Chap. VI), we
 173 write a system of renewal equations and obtain analytical formulas for the two first
 174 moments. We define $Y_t^{(j,a)} := \langle Z_t, \mathbf{1}_{j, \leq a} \rangle$ as the number of cells on layer j and of age

175 less or equal than a at time t , and $m_i^a(t)$ its mean starting from one mother cell of
176 age 0 on layer 1:

$$177 \quad (6) \quad m_j^a(t) := \mathbb{E}[Y_t^{(j,a)} | Z_0 = \delta_{1,0}].$$

178 **THEOREM 2.14.** *Under hypotheses 2.1, 2.2, 2.7, 2.8 and 2.9, for all $a \geq 0$,*

$$179 \quad (7) \quad \forall j \in \llbracket 1, J \rrbracket, \quad m_j^a(t) e^{-\lambda_c t} \rightarrow \tilde{m}_j(a), \quad t \rightarrow \infty,$$

180

181

182 where $\tilde{m}_j(a) =$

$$183 \quad \begin{cases} 0, & j \in \llbracket 1, c-1 \rrbracket, \\ \frac{\int_0^a \hat{\rho}^{(c)}(s) ds}{2p_S^{(c)} \hat{\rho}^{(c)}(0) \int_0^\infty s d\mathcal{B}_c(s) e^{-\lambda_c s} ds}, & j = c, \\ \frac{\int_0^a \hat{\rho}^{(j)}(s) ds}{2p_S^{(c)} \hat{\rho}^{(c)}(0) \int_0^\infty s d\mathcal{B}_c(s) e^{-\lambda_c s} ds} \prod_{k=1}^{c-1} \frac{2p_L^{(k)} d\mathcal{B}_k^*(\lambda_c)}{1 - 2p_S^{(k)} d\mathcal{B}_k^*(\lambda_c)}, & j \in \llbracket c+1, J \rrbracket. \end{cases}$$

184

185 **2.4.3. Calibration.** We now consider a particular choice of the division rate:

186 *Hypothesis 2.15* (Age-independent division rate). $\forall (j, a) \in \mathcal{E}$, $b_j(a) = b_j$.

187 We also consider a specific initial condition with $N \in \mathbb{N}^*$ cells:

188 *Hypothesis 2.16* (First layer initial condition). $Z_0 = N\delta_{1,0}$.

189 Then, integrating the deterministic PDE system (3) with respect to age or differenti-
190 ating the renewal equation system (see (39)) on the mean number M , we obtain:

$$191 \quad (8) \quad \begin{cases} \frac{d}{dt} M(t) = AM(t) \\ M(0) = (N, 0, \dots, 0) \in \mathbb{R}^J \end{cases}, \quad [A]_{i,j} := \begin{cases} (2p_S^{(j)} - 1)b_j, & i = j, \quad j \in \llbracket 1, J \rrbracket, \\ 2p_L^{(j-1)}b_{j-1}, & i = j-1, \quad j \in \llbracket 2, J \rrbracket. \end{cases}$$

192 We prove the structural identifiability of the parameter set $\mathbf{P} := \{N, b_j, p_S^{(j)}, j \in$
193 $\llbracket 1, J \rrbracket\}$ when we observe the vector $M(t; \mathbf{P})$ at each time t .

194 **THEOREM 2.17.** *Under hypotheses 2.1, 2.15 and 2.16 and complete observation*
195 *of system (8), the parameter set \mathbf{P} is identifiable.*

196 We then perform the estimation of the parameter set \mathbf{P} from experimental cell number
197 data retrieved on four layers and sampled at three different time points (see Table
198 1a). To improve practical identifiability, we embed biological specifications used in [1]
199 as a recurrence relation between successive division rates:

$$200 \quad (9) \quad b_j = \frac{b_1}{1 + (j-1) \times \alpha}, \quad j \in \llbracket 1, 4 \rrbracket, \quad \alpha \in \mathbb{R}.$$

201 We estimate the parameter set $\mathbf{P}_{exp} = \{N, b_1, \alpha, p_S^{(1)}, p_S^{(2)}, p_S^{(3)}\}$ using the D2D soft-
202 ware [12] with an additive Gaussian noise model (see Figure 2 and Table 1b). An
203 analysis of the profile likelihood estimate shows that all parameters except $p_S^{(2)}$ are
204 practically identifiable (see Figure SM1b).

205 **3. Theoretical proof and illustrations.**

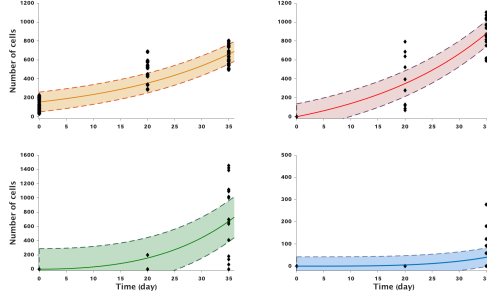


FIGURE 2. **Data fitting with model (8).** Each panel illustrates the changes in the cell number in a given layer (top-left: Layer 1, top-right: Layer 2, bottom-left: Layer 3, bottom-right: Layer 4). The black diamonds represent the experimental data, the solid lines are the best fit solutions of (8) and the dashed lines are drawn from the estimated variance. The parameter values (Table 1b) are estimated according to the procedure described in section SM2.2.

206 **3.1. Eigenproblem.** We start by solving explicitly the eigenproblem (P)-(D) to
 207 prove theorem 2.11.

208 *Proof of theorem 2.11.* According to definition 2.3, any solution of (P) in $\mathbf{L}^1(\mathbb{R}_+)^J$
 209 is given by, $\forall j \in \llbracket 1, J \rrbracket$,

$$210 \quad (10) \quad \hat{\rho}^{(j)}(a) = \hat{\rho}^{(j)}(0)e^{-\lambda a}(\mathbf{1} - \mathcal{B}_j)(a).$$

211 The boundary condition of the problem (P) gives us a system of equations for λ and
 212 $\hat{\rho}^{(j)}(0)$, $j \in \llbracket 1, J \rrbracket$:

$$213 \quad (11) \quad \hat{\rho}^{(j)}(0) \times (1 - 2p_S^{(j)} d\mathcal{B}_j^*(\lambda)) = 2p_L^{(j-1)} d\mathcal{B}_{j-1}^*(\lambda) \times \hat{\rho}^{(j-1)}(0).$$

214 This system is equivalent to

$$215 \quad C(\lambda)\hat{\rho}(0) = 0, \quad [C(\lambda)]_{i,j} = \begin{cases} 1 - 2p_S^{(j)} d\mathcal{B}_j^*(\lambda), & i = j, \quad j \in \llbracket 1, J \rrbracket, \\ 2p_L^{(j-1)} d\mathcal{B}_{j-1}^*(\lambda), & i = j - 1, \quad j \in \llbracket 2, J \rrbracket. \end{cases}$$

217 Let $\Lambda := \{\lambda_j, j \in \llbracket 1, J \rrbracket\}$. The eigenvalues of the matrix $C(\lambda)$ are $1 - 2p_S^{(j)} d\mathcal{B}_j^*(\lambda)$,
 218 $j \in \llbracket 1, J \rrbracket$. Thus, if $\lambda \notin \Lambda$, according to hypothesis 2.4, 0 is not an eigenvalue of
 219 $C(\lambda)$ which implies that $\hat{\rho}(0) = 0$. As $\hat{\rho}$ satisfies both (10) and the normalization
 220 $\llbracket \hat{\rho}, \mathbf{1} \rrbracket = 1$, we obtain a contradiction. So, necessary $\lambda \in \Lambda$.

221 We choose $\lambda = \lambda_c$ the maximum element of Λ according to hypothesis 2.7. Then,
 222 using (11) when $j = c$, we have:

$$223 \quad \hat{\rho}^{(c)}(0) \times (1 - 2p_S^{(c)} d\mathcal{B}_c^*(\lambda_c)) = 2p_L^{(c-1)} d\mathcal{B}_{c-1}^*(\lambda_c) \times \hat{\rho}^{(c-1)}(0).$$

224 Note that $1 - 2p_S^{(c)} d\mathcal{B}_c^*(\lambda_c) = 0$, so $\hat{\rho}^{(c-1)}(0) = 0$ and by backward recurrence using
 225 (11) from $j = c - 1$ to 1, it comes that $\hat{\rho}^{(j)}(0) = 0$ when $j < c$. By hypothesis 2.7,
 226 $\max(\Lambda)$ is unique. Thus, when $j > c$, $\lambda_j \neq \lambda_c$ and $1 - 2p_S^{(j)} d\mathcal{B}_j^*(\lambda_c) \neq 0$. Solving (11)
 227 from $j = c + 1$ to J , we obtain:

$$228 \quad \hat{\rho}^{(j)}(0) = \hat{\rho}^{(c)}(0) \times \prod_{k=c+1}^j \frac{2p_L^{(k-1)} d\mathcal{B}_{k-1}^*(\lambda_c)}{1 - 2p_S^{(k)} d\mathcal{B}_k^*(\lambda_c)}, \quad \forall j \in \llbracket c + 1, J \rrbracket.$$

229 We deduce $\hat{\rho}^{(c)}(0)$ from the normalization $\ll \hat{\rho}, \mathbf{1} \gg = 1$. Hence, $\hat{\rho}$ is uniquely deter-
 230 mined by (10) together with the following boundary value:

$$231 \quad (12) \quad \hat{\rho}^{(j)}(0) = \begin{cases} 0, & j \in \llbracket 1, c-1 \rrbracket, \\ \frac{1}{\sum_{j=c}^J \int_0^\infty \hat{\rho}^{(j)}(a) da \prod_{k=c+1}^j \frac{2p_L^{(k-1)} d\mathcal{B}_{k-1}^*(\lambda_c)}{1-2p_S^{(k)} d\mathcal{B}_k^*(\lambda_c)}}, & j = c, \\ \hat{\rho}^{(c)}(0) \prod_{k=c+1}^j \frac{2p_L^{(k-1)} d\mathcal{B}_{k-1}^*(\lambda_c)}{1-2p_S^{(k)} d\mathcal{B}_k^*(\lambda_c)}, & j \in \llbracket c+1, J \rrbracket. \end{cases}$$

232 For the ODE system (D), any solution is given by, for $j \in \llbracket 1, J \rrbracket$,

$$233 \quad \phi^{(j)}(a) = \left[\phi^{(j)}(0) - 2(\phi^{(j)}(0)p_S^{(j)} + \phi^{(j+1)}(0)p_L^{(j)}) \int_0^a e^{-\lambda_c s} d\mathcal{B}_j(s) ds \right] e^{\int_0^a \lambda_c + b_j(s) ds}.$$

234 As $\int_0^a b_j(s) e^{-\int_0^s \lambda_c + b_j(u) du} ds$ is equal to $d\mathcal{B}_j^*(\lambda_c) - \int_a^\infty b_j(s) e^{-\int_0^s \lambda_c + b_j(u) du} ds$, we get
 235

$$236 \quad \phi^{(j)}(a) = \left[\phi^{(j)}(0) \left(1 - 2p_S^{(j)} d\mathcal{B}_j^*(\lambda_c) + 2p_S^{(j)} \int_a^{+\infty} b_j(s) e^{-\int_0^s \lambda_c + b_j(u) du} ds \right) \right. \\ \left. - \phi^{(j+1)}(0) \left(2p_L^{(j)} d\mathcal{B}_j^*(\lambda_c) - 2p_L^{(j)} \int_a^{+\infty} b_j(s) e^{-\int_0^s \lambda_c + b_j(u) du} ds \right) \right] e^{\int_0^a \lambda_c + b_j(s) ds}.$$

239 Searching for $\phi \in \mathcal{C}_b(\mathbb{R}_+)^J$, it comes that

$$240 \quad (13) \quad \forall j \in \llbracket 1, J \rrbracket, \quad \phi^{(j)}(0) \left(1 - 2p_S^{(j)} d\mathcal{B}_j^*(\lambda_c) \right) - \phi^{(j+1)}(0) 2p_L^{(j)} d\mathcal{B}_j^*(\lambda_c) = 0.$$

241 According to definition 2.4, when $j = c$ in (13) we get $\phi^{(c+1)}(0) = 0$. Recursively,
 242 $\phi^{(j)}(0) = 0$ when $j > c$. Solving (13) from $j = 1$ to $c-1$, we get

$$243 \quad (14) \quad \forall j \in \llbracket 1, c-1 \rrbracket, \quad \phi^{(j)}(0) = \phi^{(c)}(0) \times \prod_{k=j}^{c-1} \frac{2p_L^{(k-1)} d\mathcal{B}_{k-1}^*(\lambda_c)}{1-2p_S^{(k)} d\mathcal{B}_k^*(\lambda_c)}.$$

244 Again, we deduce $\phi^{(c)}(0)$ from the normalization $1 = \ll \hat{\rho}, \phi \gg = \langle \hat{\rho}^{(c)}, \phi^{(c)} \rangle$. Using
 245 corollary 2.10, we apply Fubini theorem:

$$246 \quad (15) \quad \phi^{(c)}(0) = \frac{1}{2\hat{\rho}^{(c)}(0)p_S^{(c)} \int_0^\infty \left(\int_a^{+\infty} e^{-\lambda_c s} d\mathcal{B}_c(s) ds \right) da} = \frac{1}{2\hat{\rho}^{(c)}(0)p_S^{(c)} \int_0^\infty s e^{-\lambda_c s} d\mathcal{B}_c(s) ds}.$$

247 Hence, the dual function ϕ is uniquely determined by

$$248 \quad (16) \quad \phi^{(j)}(a) = 2 \left[p_S^{(j)} \phi^{(j)}(0) + p_L^{(j)} \phi^{(j+1)}(0) \right] \int_a^{+\infty} b_j(s) e^{-\int_a^s \lambda_c + b_j(u) du} ds.$$

249 together with the boundary value (14) and (15) (ϕ is null on the layers upstream the
 250 leading layer). \square

251 From theorem 2.11, we deduce the following bounds on ϕ (see proof in SM1.1).

252 **COROLLARY 3.1.** *According to hypotheses 2.2, 2.4 and 2.7,*

$$253 \quad (17) \quad \forall j \in \llbracket 1, J \rrbracket, \quad \frac{\underline{b}_j}{\lambda_c + \underline{b}_j} \leq \frac{\phi^{(j)}(a)}{2[p_S^{(j)} \phi^{(j)}(0) + p_L^{(j)} \phi^{(j+1)}(0)]} \leq 1.$$

254 To conclude this section, we also solve the additional dual problem on isolated layers
255 which is needed to obtain the large-time convergence (see proof in SM1.1).

256 LEMMA 3.2. *According to hypotheses 2.2, 2.4 and 2.9, any solution $\hat{\phi}$ of (4) sat-*
257 *isfies*

$$258 \quad (18) \quad \forall j \in \llbracket 1, J \rrbracket, \quad \hat{\phi}^{(j)}(a) = 2p_S^{(j)} \hat{\phi}^{(j)}(0) \int_a^{+\infty} b_j(s) e^{-\lambda_j s - \int_a^s b_j(u) du} ds$$

$$259 \quad \text{and, } \forall a \in \mathbb{R}_+ \cup \{+\infty\}, \quad \frac{\bar{b}_j}{\lambda_j + \bar{b}_j} \leq \frac{\hat{\phi}^{(j)}(a)}{2p_S^{(j)} \hat{\phi}^{(j)}(0)} < +\infty.$$

260 In all the sequel, we fix

$$261 \quad (19) \quad \hat{\phi}^{(c)}(0) = \phi^{(c)}(0), \quad \forall j \in \llbracket 1, c-1 \rrbracket \quad \hat{\phi}^{(j)}(0) = \phi^{(j)}(0) + \frac{p_L^{(j)}}{p_S^{(j)}} \phi^{(j+1)}(0).$$

262 A first consequence is that $\hat{\phi}^{(c)} = \phi^{(c)}$ and moreover, from corollary 3.1 and lemma
263 3.2, we have

$$264 \quad (20) \quad \phi^{(j)}(a) \leq \frac{\lambda_j + \bar{b}_j}{\bar{b}_j} \hat{\phi}^{(j)}(a).$$

265 **3.2. Asymptotic study for the deterministic formalism.** Adapting the
266 method of characteristic, it is classical to construct the unique solution in
267 $\mathcal{C}^1(\mathbb{R}_+, \mathbf{L}^1(\mathbb{R}_+)^J)$ of (3) ([16], Chap. I). Let ρ the solution of (3), $\hat{\rho}$ and ϕ given by
268 theorem 2.11 and $\eta = \ll \rho_0, \phi \gg$. We define h as

$$269 \quad (21) \quad h(t, a) = e^{-\lambda_c t} \rho(t, a) - \eta \hat{\rho}(a), \quad (t, a) \in \mathbb{R}_+ \times \mathbb{R}_+.$$

270 Following [7], we first show a conservation principle (see proof in SM1.1).

LEMMA 3.3 (Conservation principle). *The function h satisfies the conservation principle*

$$\ll h(t, \cdot), \phi \gg = 0.$$

271 Secondly, we prove that h is solution of the following PDE system (see proof in SM1.1).

272 LEMMA 3.4. *h is solution of*

$$273 \quad (22) \quad \begin{cases} \partial_t |h(t, a)| + \partial_a |h(t, a)| + (\lambda_c + B(a)) |h(t, a)| = 0, \\ |h(t, 0)| = \left| \int_0^{+\infty} K(a) h(t, a) da \right|. \end{cases}$$

274 Together with the above lemmas 3.2, 3.3 and 3.4, we now prove the following key
275 estimates required for the asymptotic behavior.

276 LEMMA 3.5. *$\forall j \in \llbracket 1, J \rrbracket$, the component $h^{(j)}$ of h verifies the inequality*

$$277 \quad (23) \quad \partial_t \langle |h^{(j)}(t, \cdot)|, \hat{\phi}^{(j)} \rangle \leq \alpha_{j-1} \langle |h^{(j-1)}(t, \cdot)|, \hat{\phi}^{(j-1)} \rangle - \mu_j \langle |h^{(j)}(t, \cdot)|, \hat{\phi}^{(j)} \rangle + r_j(t),$$

278 where $\alpha_0 := 0$, for $j \in \llbracket 1, J \rrbracket$, $\alpha_j := \frac{p_L^{(j)} \bar{b}_j}{p_S^{(j)} \bar{b}_j} \frac{\hat{\phi}^{(j+1)}(0)}{\hat{\phi}^{(j)}(0)} (\lambda_j + \bar{b}_j)$ and

$$279 \quad \mu_j = \begin{cases} 0, & j \neq c \\ \lambda_c - \lambda_j, & j \neq c \\ \bar{b}_c, & j = c \end{cases}, \quad r_j(t) := \begin{cases} 0, & j \neq c \\ \sum_{j=1}^{c-1} \frac{\lambda_j + \bar{b}_j}{\bar{b}_j} \langle |h^{(j)}(t, \cdot)|, \hat{\phi}^{(j)} \rangle, & j = c. \end{cases}$$

314 As before, using lemma 3.2, we obtain

$$315 \quad 2p_L^{(c-1)} \hat{\phi}^{(c)}(0) \left| \left\langle h^{(c-1)}(t, \cdot), b_{c-1} \right\rangle \right| \leq \alpha_{c-1} \left\langle |h^{(c-1)}(t, \cdot)|, \hat{\phi}^{(c-1)} \right\rangle.$$

316 Combining the latter inequality with (30) and (26), we deduce (23) for $j = c$. \square

317 We now have all the elements to prove theorem 2.12.

318 *Proof of theorem 2.12.* We proceed by recurrence from the index $j = 1$ to J . For
319 $j = 1$, we can apply Gronwall lemma in inequality (23) to get

$$320 \quad \left\langle |h^{(1)}(t, \cdot)|, \hat{\phi}^{(1)} \right\rangle \leq e^{-\mu_1 t} \left\langle |h^{(1)}(0, \cdot)|, \hat{\phi}^{(1)} \right\rangle.$$

321 We suppose that for a fixed $2 \leq j \leq J$ and for all ranks $1 \leq i \leq j - 1$, there exist
322 polynomials $\beta_k^{(i)}$, $k \in \llbracket 1, i \rrbracket$, of degree at most $i - k$ such that

$$323 \quad (31) \quad \left\langle |h^{(i)}(t, \cdot)|, \hat{\phi}^{(i)} \right\rangle \leq \sum_{k=1}^i \beta_k^{(i)}(t) e^{-\mu_k t} \left\langle |h^{(k)}(0, \cdot)|, \hat{\phi}^{(k)} \right\rangle.$$

325 Applying this recurrence hypothesis in inequality (23) for j , there exist polynomials
326 $\tilde{\beta}_k^{(j)}(t)$ for $k \in \llbracket 1, j - 1 \rrbracket$ (same degree than $\beta_k^{(j-1)}(t)$):

$$327 \quad \partial_t \left\langle |h^{(j)}(t, \cdot)|, \hat{\phi}^{(j)} \right\rangle \leq \sum_{k=1}^{j-1} \tilde{\beta}_k^{(j)}(t) e^{-\mu_k t} \left\langle |h^{(k)}(0, \cdot)|, \hat{\phi}^{(k)} \right\rangle - \mu_j \left\langle |h^{(j)}(t, \cdot)|, \hat{\phi}^{(j)} \right\rangle.$$

328 We get from a modified version of Gronwall lemma (see lemma SM1.1):

$$329 \quad \left\langle |h^{(j)}(t, \cdot)|, \hat{\phi}^{(j)} \right\rangle \leq \sum_{k=1}^j \beta_k^{(j)}(t) e^{-\mu_k t} \left\langle |h^{(k)}(0, \cdot)|, \hat{\phi}^{(k)} \right\rangle.$$

330 where $\beta_j^{(j)}$ is a constant and for $k \in \llbracket 1, j - 1 \rrbracket$, $\beta_k^{(j)}$ is a polynomial of degree at most
331 $(j - 1 - k) + 1 = j - k$ (the degree only increases by 1 when $\mu_k = \mu_j$). This achieves
332 the recurrence. \square

333 **3.3. Asymptotic study of the martingale problem.** The existence and
334 uniqueness of the SDE (2) is proved in a more general context than ours in [15].
335 Following the approach proposed in [15], we first derive the generator of the process
336 Z solution of (2). In this part, we consider $F \in \mathcal{C}^1(\mathbb{R}_+, \mathbb{R}_+)$ and $f \in \mathcal{C}_b^1(\mathcal{E}, \mathbb{R}_+)$.

337 **THEOREM 3.6** (Infinitesimal generator of (Z_t)). *Under hypotheses 2.1 and 2.2,*
338 *the process Z defined in (2) and starting from Z_0 is a Markovian process in the Skhovor*
339 *space $\mathbb{D}([0, T], \mathcal{M}_P(\llbracket 1, J \rrbracket \times \mathbb{R}_+))$. Let $T > 0$, Z satisfies*

$$340 \quad (32) \quad \mathbb{E} \left[\sup_{t \leq T} N_t \right] < \infty, \quad \mathbb{E} \left[\sup_{t \leq T} \ll a, Z_t \gg \right] < \infty,$$

341 and its infinitesimal generator is

$$\begin{aligned}
& \mathcal{G}F[\ll f, Z \gg] = \ll F'[\ll Z, f \gg] \partial_a f, Z \gg \\
& + \sum_{j=1}^J \int_0^\infty (F[\ll f, 2\delta_{j,0} - \delta_{j,a} + Z \gg] - F[\ll f, Z \gg]) p_{2,0}^{(j)} b_j(a) Z(dj, da) \\
342 & + \sum_{j=1}^J \int_0^\infty (F[\ll f, \delta_{j,0} + \delta_{j+1,0} - \delta_{j,a} + Z \gg] - F[\ll f, Z \gg]) p_{1,1}^{(j)} b_j(a) Z(dj, da) \\
& + \sum_{j=1}^J \int_0^\infty (F[\ll f, 2\delta_{j+1,0} - \delta_{j,a} + Z \gg] - F[\ll f, Z \gg]) p_{0,2}^{(j)} b_j(a) Z(dj, da).
\end{aligned}$$

343 From this theorem, we derive the following Dynkin formula :

344 LEMMA 3.7 (Dynkin formula). *Let $T > 0$. Under hypotheses 2.1 and 2.2, $\forall t \in$*
345 $[0, T]$,

$$346 \quad F[\ll f, Z_t \gg] = F[\ll f, Z_0 \gg] + \int_0^t \mathcal{G}F[\ll f, Z_s \gg] ds + M_t^{F,f}$$

347 where $M^{F,f}$ is a martingale. Moreover,

$$348 \quad (33) \quad \ll f, Z_t \gg = \ll f, Z_0 \gg + \int_0^t \ll \mathcal{L}^D f, Z_s \gg ds + M_t^f$$

349 where \mathcal{L}^D the dual operator in (D) and M^f is a \mathbf{L}^2 -martingale defined by
350 (34)

$$\begin{aligned}
M_t^f &= \int_0^t \ll B(\cdot) f(\cdot) - K(\cdot)^T f(0), Z_s \gg ds \\
&+ \int \int_{[0,t] \times \mathcal{E}} \mathbf{1}_{k \leq N_{s^-}} \ll f, 2\delta_{I_{s^-}^{(k)}, 0} - \delta_{I_{s^-}^{(k)}, A_{s^-}^{(k)}} \gg \mathbf{1}_{0 \leq \theta \leq m_1(s,k,Z)} Q(ds, dk, d\theta) \\
351 &+ \int \int_{[0,t] \times \mathcal{E}} \mathbf{1}_{k \leq N_{s^-}} \ll f, \delta_{I_{s^-}^{(k)}, 0} + \delta_{I_{s^-}^{(k)}+1, 0} - \delta_{I_{s^-}^{(k)}, A_{s^-}^{(k)}} \gg \mathbf{1}_{m_1(s,k,Z) \leq \theta \leq m_2(s,k,Z)} Q(ds, dk, d\theta) \\
&+ \int \int_{[0,t] \times \mathcal{E}} \mathbf{1}_{k \leq N_{s^-}} \ll f, 2\delta_{I_{s^-}^{(k)}+1, 0} - \delta_{I_{s^-}^{(k)}, A_{s^-}^{(k)}} \gg \mathbf{1}_{m_2(s,k,Z) \leq \theta \leq m_3(s,k,Z)} Q(ds, dk, d\theta)
\end{aligned}$$

351 and

$$\begin{aligned}
\langle M^f, M^f \rangle_t &= \int_0^t \left[\sum_{j=1}^J \int_{\mathbb{R}_+} [\ll f, 2\delta_{j,0} - \delta_{j,a} \gg]^2 b_j(a) p_{2,0}^{(j)} Z_s(dj, da) \right. \\
352 \quad (35) &+ \sum_{j=1}^J \int_{\mathbb{R}_+} [\ll f, \delta_{j,0} + \delta_{j+1,0} - \delta_{j,a} \gg]^2 b_j(a) p_{1,1}^{(j)} Z_s(dj, da) \\
&+ \left. \sum_{j=1}^J \int_{\mathbb{R}_+} [\ll f, 2\delta_{j+1,0} - \delta_{j,a} \gg]^2 b_j(a) p_{0,2}^{(j)} Z_s(dj, da) \right] ds.
\end{aligned}$$

353 The proofs of theorem 3.6 and lemma 3.7 are classical and provided in SM1.2 for
354 reader convenience. We now have all the elements to prove theorem 2.13.

355 *Proof of theorem 2.13.* We apply the Dynkin formula (33) with the dual test func-
356 tion ϕ and obtain $\ll \phi, Z_t \gg = \ll \phi, Z_0 \gg + \lambda_c \int_0^t \ll \phi, Z_s \gg ds + M_t^\phi$. As ϕ is
357 bounded, $\ll \phi, Z_t \gg$ has finite expectation for all time t according to (32). Thus,

$$358 \quad (36) \quad \mathbb{E}[\ll \phi, Z_t \gg] = \mathbb{E}[\ll \phi, Z_0 \gg] + \lambda_c \mathbb{E}\left[\int_0^t \ll \phi, Z_s \gg ds\right].$$

359 Using Fubini theorem and solving equation (36), we obtain:

$$360 \quad \mathbb{E}[\langle\langle \phi, Z_t \rangle\rangle] = e^{\lambda_c t} \mathbb{E}[\langle\langle \phi, Z_0 \rangle\rangle] \Rightarrow \mathbb{E}[e^{-\lambda_c t} \langle\langle \phi, Z_t \rangle\rangle] = \mathbb{E}[\langle\langle \phi, Z_0 \rangle\rangle].$$

361 Hence, $W_t^\phi = e^{-\lambda_c t} \langle\langle \phi, Z_t \rangle\rangle$ is a martingale. According to martingale convergence
 362 theorems (see Theorem 7.11 in [4]), W_t^ϕ converges to an integrable random variable
 363 $W_\infty^\phi \geq 0$, \mathbb{P} -p.s. when t goes to infinity. To prove that W_∞^ϕ is non-degenerated,
 364 we will show that the convergence holds in \mathbf{L}^2 . Indeed, from the \mathbf{L}^2 and almost
 365 sure convergence, we deduce the \mathbf{L}^1 convergence. Then, applying the dominated
 366 convergence theorem, we have:

$$367 \quad \mathbb{E}[W_\infty^\phi] := \mathbb{E}[\lim_{t \rightarrow \infty} W_t^\phi] = \lim_{t \rightarrow \infty} \mathbb{E}[W_t^\phi] = \mathbb{E}[W_0^\phi] > 0.$$

368 Consequently, W_∞^ϕ is non-degenerated. To show the \mathbf{L}^2 convergence, we compute the
 369 quadratic variation of W^ϕ . Applying Ito formula (see [10] p. 78-81) with $F(t, \langle\langle$
 370 $\phi, Z_t \rangle\rangle) = e^{-\lambda_c t} \langle\langle \phi, Z_t \rangle\rangle$, we deduce:

$$\begin{aligned} W_t^\phi &= \langle\langle \phi, Z_0 \rangle\rangle + \int_0^t \left[\int_{\mathcal{E}} e^{-\lambda_c s} (\partial_a \phi^{(j)}(a) - \lambda_c \phi^{(j)}(a)) Z_s(dj, da) \right] ds \\ &+ \int \int_{[0,t] \times \mathcal{E}} \mathbb{1}_{k \leq N_{s^-}} e^{-\lambda_c s} \langle\langle \phi, 2\delta_{I_{s^-}, 0} - \delta_{I_{s^-}, A_{s^-}^{(k)}} \rangle\rangle \mathbb{1}_{0 \leq \theta \leq m_1(s, k, Z)} Q(ds, dk, d\theta) \\ 371 &+ \int \int_{[0,t] \times \mathcal{E}} \mathbb{1}_{k \leq N_{s^-}} e^{-\lambda_c s} \langle\langle \phi, \delta_{I_{s^-}, 0} + \delta_{I_{s^-}, +1, 0} - \delta_{I_{s^-}, A_{s^-}^{(k)}} \rangle\rangle \mathbb{1}_{m_1(s, k, Z) \leq \theta \leq m_2(s, k, Z)} Q(ds, dk, d\theta) \\ &+ \int \int_{[0,t] \times \mathcal{E}} \mathbb{1}_{k \leq N_{s^-}} e^{-\lambda_c s} \langle\langle \phi, 2\delta_{I_{s^-}, +1, 0} - \delta_{I_{s^-}, A_{s^-}^{(k)}} \rangle\rangle \mathbb{1}_{m_2(s, k, Z) \leq \theta \leq m_3(s, k, Z)} Q(ds, dk, d\theta). \end{aligned}$$

372 As $\mathcal{L}^D \phi = \lambda_c \phi$, we have

$$373 \quad \int_{\mathcal{E}} (\partial_a \phi^{(j)}(a) - \lambda_c \phi^{(j)}(a)) Z_s(dj, da) = \langle\langle B(\cdot) \phi(\cdot) - K^T(\cdot) \phi(0), Z_s \rangle\rangle .$$

375 Consequently, from (34), we deduce

$$376 \quad (37) \quad W_t^\phi = \langle\langle \phi, Z_0 \rangle\rangle + \int_0^t e^{-\lambda_c s} dM_s^\phi .$$

377 where dM_s^ϕ is defined as $M_t^\phi = \int_0^t dM_s^\phi$. According to (35) and (37), we get

$$\begin{aligned} 378 \quad \langle W^\phi, W^\phi \rangle_t &= \int_0^t e^{-2\lambda_c s} d \langle M^\phi, M^\phi \rangle_s ds \\ 379 &= \int_0^t e^{-2\lambda_c s} \left[\int_{\mathcal{E}} \left(p_{2,0}^{(j)} [\langle\langle \phi, 2\delta_{j,0} - \delta_{j,a} \rangle\rangle]^2 + p_{1,1}^{(j)} [\langle\langle \phi, \delta_{j,0} + \delta_{j+1,0} - \delta_{j,a} \rangle\rangle]^2 \right. \right. \\ 380 &\quad \left. \left. + p_{0,2}^{(j)} [\langle\langle \phi, 2\delta_{j+1,0} - \delta_{j,a} \rangle\rangle]^2 \right) b_j(a) Z_s(dj, da) \right] ds . \end{aligned}$$

383 Since, ϕ and b are bounded, there exists a constant $K > 0$ such that

$$384 \quad \langle W^\phi, W^\phi \rangle_t \leq K \int_0^t e^{-2\lambda_c s} \left[\int_{\mathcal{E}} Z_s(dj, da) \right] ds .$$

385 Taking the expectation and using moment estimate (32), we get $\mathbb{E}[\langle W^\phi, W^\phi \rangle_t] < \infty$.

386 Thanks to the Burkholder-Davis-Gundy inequality (see Theorem 48, [10]), we deduce

387 that $\mathbb{E}[\sup_{t \leq T} (W_t^\phi)^2] < \infty$, and thus the \mathbf{L}^2 convergence of W^ϕ . \square

388 **3.4. Asymptotic study of the renewal equations.** We now turn to the study
 389 of renewal equations associated with the branching process Z . Following [2] (Chap.
 390 VI), we introduce generating functions that determine the cell moments. In all this
 391 subsection, we consider $a \in \mathbb{R}_+ \cup \{+\infty\}$. We recall that $Y_t^{(j,a)} = \langle Z_t, \mathbb{1}_j \mathbb{1}_{\leq a} \rangle$ and
 392 $Y_t^a = (Y_t^{(j,a)})_{j \in \llbracket 1, J \rrbracket}$. For $\mathbf{s} = (s_1, \dots, s_J) \in \mathbb{R}^J$ and $\mathbf{j} = (j_1, \dots, j_J) \in \mathbb{N}^J$, we use
 393 classical vector notation $\mathbf{s}^{\mathbf{j}} = \prod_{i=1}^J s_i^{j_i}$.

DEFINITION 3.8. We define $F^a[\mathbf{s}; t] = (F^{(i,a)}[\mathbf{s}; t])_{i \in \llbracket 1, J \rrbracket}$ where $F^{(i,a)}$ is the generating function associated with Y_t^a starting with $Z_0 = \delta_{i,0}$:

$$F^{(i,a)}[\mathbf{s}; t] := \mathbb{E}[\mathbf{s}^{Y_t^a} | Z_0 = \delta_{i,0}].$$

394 We obtain a system of renewal equations for F and

$$395 M^a(t) := (\mathbb{E}[Y_t^{(j,a)} | Z_0 = \delta_{i,0}])_{i,j \in \llbracket 1, J \rrbracket}.$$

396 LEMMA 3.9 (Renewal equations for F). For $i \in \llbracket 1, J \rrbracket$, $F^{(i,a)}$ satisfies:

$$397 (38) \quad \forall i \in \llbracket 1, J \rrbracket, \quad F^{(i,a)}[\mathbf{s}; t] = (s_i \mathbb{1}_{t \leq a} + \mathbb{1}_{t > a})(1 - \mathcal{B}_i(t)) + f^{(i)}(F^a[\mathbf{s}, \cdot]) * d\mathcal{B}_i(t)$$

398 where $f^{(i)}$ is given by $f^{(i)}(\mathbf{s}) := p_{2,0}^{(i)} s_i^2 + p_{1,1}^{(i)} s_i s_{i+1} + p_{0,2}^{(i)} s_{i+1}^2$.

399 LEMMA 3.10 (Renewal equations for M). For $(i, j) \in \llbracket 1, J \rrbracket^2$, $M_{i,j}^a$ satisfies:

$$400 (39) \quad M_{i,j}^a(t) = \delta_{i,j}(1 - \mathcal{B}_i(t)) \mathbb{1}_{t \leq a} + 2p_S^{(i)} M_{i,j}^a * d\mathcal{B}_i(t) + 2p_L^{(i)} M_{i+1,j}^a * d\mathcal{B}_i(t).$$

401 The proofs of lemma 3.9 and 3.10 are given in SM1.2.

402 THEOREM 3.11. Under hypotheses 2.1, 2.2, 2.7, 2.8 and 2.9,

$$403 (40) \quad \forall i \in \llbracket 1, J \rrbracket, \quad \forall k \in \llbracket 0, J - i \rrbracket, \quad M_{i,i+k}^a(t) \sim \widetilde{M}_{i,i+k}(a) e^{\lambda_{i,i+k} t}, \quad t \rightarrow \infty$$

404 where $\lambda_{i,i+k} = \max_{j \in \llbracket i, i+k \rrbracket} \lambda_j$,

$$405 (41) \quad \widetilde{M}_{i,i}(a) = \frac{\int_0^a (1 - \mathcal{B}_i(t)) e^{-\lambda_i t} dt}{2p_S^{(i)} \int_0^\infty t d\mathcal{B}_i(t) e^{-\lambda_i t} dt}$$

406 and, for $k \in \llbracket 1, J - i \rrbracket$

$$407 (42) \quad \widetilde{M}_{i,i+k}(a) = \begin{cases} \frac{2p_L^{(i)} d\mathcal{B}_i^*(\lambda_{i,i+k})}{1 - 2p_S^{(i)} d\mathcal{B}_i^*(\lambda_{i,i+k})} \widetilde{M}_{i+1,i+k}(a), & \text{if } \lambda_{i,i+k} \neq \lambda_i(i) \\ \frac{2p_L^{(i)} d\mathcal{B}_i^*(\lambda_i)}{2p_S^{(i)} \int_0^\infty t d\mathcal{B}_i(t) e^{-\lambda_i t} dt} \int_0^\infty M_{i+1,i+k}^a(t) e^{-\lambda_i t} dt, & \text{if } \lambda_{i,i+k} = \lambda_i(ii). \end{cases}$$

408 *Proof.* Let the mother cell index $i \in \llbracket 1, J \rrbracket$. As no daughter cell can move up-
 409 stream to its mother layer, the mean number of cells on layer $j < i$ is null (for all
 410 $t \geq 0$ and for $j < i$, $M_{i,j}^a(t) = 0$). We consider the layers downstream the mother one
 411 ($j \geq i$) and proceed by recurrence:

$$412 \mathcal{H}^k : \quad \forall i \in \llbracket 1, J - k \rrbracket, \quad M_{i,i+k}^a(t) \sim \widetilde{M}_{i,i+k}(a) e^{\lambda_{i,i+k} t}, \quad \text{as } t \rightarrow \infty.$$

413 We first deal with \mathcal{H}^0 . We consider the solution of (39) for $j = i$:

$$414 \quad (43) \quad \forall t \in \mathbb{R}_+, \quad M_{i,i}^a(t) = (1 - \mathcal{B}_i(t)) \mathbf{1}_{t \leq a} + 2p_S^{(i)} M_{i,i}^a * d\mathcal{B}_i(t).$$

415 We recognize a renewal equation as presented in [2](p.161, eq.(1)) for $M_{i,i}$, which is
 416 similar to a single type age-dependent process. The main results on renewal equations
 417 are recalled in SM1.3. Here, the mean number of children is $m = 2p_S^{(i)} > 0$ and the
 418 life time distribution is \mathcal{B}_i . From hypothesis 2.2, we have

$$419 \quad \int_0^\infty (1 - \mathcal{B}_i(t)) \mathbf{1}_{t \leq a} e^{-\lambda_i t} dt \leq \frac{1}{b_i} \int_0^\infty \mathbf{1}_{t \leq a} d\mathcal{B}_i(t) e^{-\lambda_i t} dt \leq \frac{1}{b_i} \int_0^\infty d\mathcal{B}_i(t) e^{-\lambda_i t} dt < \infty$$

420 according to hypothesis 2.4. Thus, $t \mapsto \mathbf{1}_{t \leq a} (1 - \mathcal{B}_i(t)) e^{-\lambda_i t}$ is in $\mathbf{L}^1(\mathbb{R}_+)$. Using
 421 hypotheses 2.4 and 2.9, we apply corollary 2.10 and lemma SM1.4 (see lemma 2 of
 422 [2],p.161) and obtain:

$$423 \quad M_{i,i}^a(t) \sim \widetilde{M}_{i,i}(a) e^{\lambda_i t}, \text{ as } t \rightarrow \infty, \text{ where } \widetilde{M}_{i,i}(a) = \frac{\int_0^a (1 - \mathcal{B}_i(t)) e^{-\lambda_i t} dt}{2p_S^{(i)} \int_0^\infty t d\mathcal{B}_i(t) e^{-\lambda_i t} dt}.$$

424 Hence, \mathcal{H}^0 is verified. We then suppose that \mathcal{H}^{k-1} is true for a given rank $k - 1 \geq 0$
 425 and consider the next rank k . According to (39), $M_{i,i+k}^a$ is a solution of the equation:

$$426 \quad (44) \quad M_{i,i+k}^a(t) = 2p_S^{(i)} M_{i,i+k}^a * d\mathcal{B}_i(t) + 2p_L^{(i)} M_{i+1,i+k}^a * d\mathcal{B}_i(t).$$

427 We distinguish two cases : $\lambda_{i,i+k} \neq \lambda_i$ and $\lambda_{i,i+k} = \lambda_i$. We first consider $\lambda_{i,i+k} = \lambda_i$
 428 and show that $f(t) = M_{i+1,i+k}^a * d\mathcal{B}_i(t) e^{-\lambda_i t}$ belongs to $\mathbf{L}^1(\mathbb{R}_+)$. Let $R > 0$. Using
 429 Fubini theorem, we deduce that:

$$430 \quad \int_0^R f(t) dt = \int_0^R \left[\int_u^R e^{-\lambda_i(t-u)} M_{i+1,i+k}^a(t-u) dt \right] e^{-\lambda_i u} d\mathcal{B}_i(u) du.$$

431 Applying a change of variable and using that $M_{i+1,i+k}^a(t) \geq 0$ for all $t \geq 0$, we have:

$$432 \quad \int_u^R e^{-\lambda_i(t-u)} M_{i+1,i+k}^a(t-u) dt \leq \int_0^R e^{-\lambda_i t} M_{i+1,i+k}^a(t) dt.$$

433 According to \mathcal{H}^k , we know that $M_{i+1,i+k}^a(t) \sim \widetilde{M}_{i+1,i+k}(a) e^{\lambda_{i+1,i+k} t}$ as $t \rightarrow \infty$. Then,
 434

$$435 \quad \int_0^R e^{-\lambda_i t} M_{i+1,i+k}^a(t) dt = \int_0^R e^{-\lambda_{i+1,i+k} t} M_{i+1,i+k}^a(t) e^{-(\lambda_i - \lambda_{i+1,i+k}) t} dt \\ 436 \quad \leq K \int_0^R e^{-(\lambda_i - \lambda_{i+1,i+k}) t} dt < \infty$$

438 when $R \rightarrow \infty$, as $\lambda_i = \lambda_{i,i+k} > \lambda_{i+1,i+k}$. Moreover, $\int_0^R e^{-\lambda_i u} d\mathcal{B}_i(u) du \leq d\mathcal{B}_i^*(\lambda_i) <$
 439 ∞ according to hypothesis 2.7. Finally, we obtain an estimate for $\int_0^R f(t) dt$ that
 440 does not depend on R . So, f is integrable. We can apply lemma SM1.4 and deduce
 441 $M_{i,i+k}^a(t) \sim \widetilde{M}_{i,i+k}(a) e^{\lambda_{i,i+k} t}$, as $t \rightarrow \infty$, with $\widetilde{M}_{i,i+k}(a)$ given in (42)(ii).

442 We now consider the case $\lambda_{i,i+k} \neq \lambda_i$ and introduce the following notations :

$$443 \quad \widehat{M}_{i,i+k}^a(t) = M_{i,i+k}^a(t) e^{-\lambda_{i,i+k} t}, \quad \widehat{d\mathcal{B}_i}(t) = \frac{d\mathcal{B}_i(t)}{d\mathcal{B}_i^*(\lambda_{i,i+k})} e^{-\lambda_{i,i+k} t}.$$

444 In this case, $\lambda_{i,i+k} > \lambda_i$, so that $2p_S^{(i)} d\mathcal{B}_i^*(\lambda_{i,i+k}) < 2p_S^{(i)} d\mathcal{B}_i^*(\lambda_i) = 1$. We want to
 445 apply lemma SM1.5 (see lemma 4 of [2], p.163). We rescale (44) by $e^{-\lambda_{i,i+k}t}$ and
 446 obtain the following renewal equation for $\widehat{M}_{i,i+1}^a$:

$$447 \quad \widehat{M}_{i,i+k}^a(t) = 2p_S^{(i)} d\mathcal{B}_i^*(\lambda_{i,i+k}) \widehat{M}_{i,i+k}^a * \widehat{d\mathcal{B}_i}(t) + 2p_L^{(i)} M_{i+1,i+k}^a * d\mathcal{B}_i(t) e^{-\lambda_{i,i+k}t}.$$

448 We compute the limit of $f(t) = M_{i+1,i+k}^a * d\mathcal{B}_i(t) e^{-\lambda_{i,i+k}t}$:

$$449 \quad f(t) = \int_0^\infty \mathbb{1}_{[0,t]}(u) M_{i+1,i+k}^a(t-u) e^{-\lambda_{i,i+k}(t-u)} e^{-\lambda_{i,i+k}u} d\mathcal{B}_i(u) du.$$

450 According to \mathcal{H}^{k-1} , $M_{i+1,i+k}^a(t) \sim e^{-\lambda_{i+1,i+k}t} \widetilde{M}_{i+1,i+k}(a)$. As $\lambda_{i,i+k} \neq \lambda_i$, we have
 451 $\lambda_{i,i+k} = \lambda_{i+1,i+k}$. Hence, $M_{i+1,i+k}^a(t) e^{-\lambda_{i,i+k}t}$ is dominated by a constant K such
 452 that $\int_0^\infty K e^{-\lambda_{i,i+k}u} d\mathcal{B}_i(u) du < \infty$. We apply the Lebesgue dominated convergence
 453 theorem and obtain $\lim_{t \rightarrow \infty} f(t) = \widetilde{M}_{i+1,i+k}(a) d\mathcal{B}_i^*(\lambda_{i,i+k})$. Applying lemma SM1.5, we
 454 obtain that:

$$455 \quad \lim_{t \rightarrow \infty} \widehat{M}_{i,i+k}^a(t) = \frac{2p_L^{(i)} \widetilde{M}_{i+1,i+k}(a) d\mathcal{B}_i^*(\lambda_{i,i+k})}{1 - 2p_S^{(i)} d\mathcal{B}_i^*(\lambda_{i,i+k})} = \widetilde{M}_{i,i+k}(a),$$

456 and the recurrence is proved. \square

457 We have now all the elements to prove theorem 2.14.

458 *Proof of theorem 2.14.* According to theorem 3.11, we have:

$$459 \quad (45) \quad \forall j \in \llbracket 1, J \rrbracket, \quad m_j^a(t) \sim \widetilde{M}_{1,j}(a) e^{\lambda_{1,j}t}, \quad \text{as } t \rightarrow \infty.$$

460 When $j < c$, we deduce directly from (45) that $\widetilde{m}_j(a) = 0$. We then consider the
 461 leading layer $j = c$. For $k \in \llbracket 1, c-1 \rrbracket$, $\lambda_{k,c} \neq \lambda_k$ so, $\widetilde{M}_{k,c}(a)$ is related to $\widetilde{M}_{k+1,c}(a)$
 462 by (42)(i). Thus, we obtain:

$$463 \quad (46) \quad \widetilde{m}_c(a) = \prod_{m=1}^{c-1} \frac{2p_L^{(m)} d\mathcal{B}_m^*(\lambda_c)}{1 - 2p_S^{(m)}(d\mathcal{B}_m^*)(\lambda_c)} \widetilde{M}_{c,c}(a).$$

464 $\widetilde{M}_{c,c}(a)$ is given by (41) and we deduce $\widetilde{m}_c(a)$. We turn to the layers $j > c$. For
 465 $k \in \llbracket 1, c-1 \rrbracket$, we have $\lambda_c = \lambda_{k,j} \neq \lambda_k$. We obtain from (42)(i)

$$466 \quad (47) \quad \widetilde{m}_j(a) = \prod_{m=1}^{c-1} \frac{2p_L^{(m)} d\mathcal{B}_m^*(\lambda_c)}{1 - 2p_S^{(m)}(d\mathcal{B}_m^*)(\lambda_c)} \widetilde{M}_{c,j}(a).$$

467 Then, as $\lambda_c = \lambda_{c,j}$, we use (42)(ii) and obtain:

$$468 \quad (48) \quad \widetilde{M}_{c,j}(a) = \frac{2p_L^{(c)} d\mathcal{B}_c^*(\lambda_c)}{2p_S^{(c)} \int_0^\infty t e^{-\lambda_c t} d\mathcal{B}_c(t)} \int_0^\infty M_{c+1,j}^a(t) e^{-\lambda_c t} dt.$$

469 Then, we apply the Laplace transform to (39) for $\alpha = \lambda_c$. Theorem 3.11 and the fact
 470 that $\lambda_c = \lambda_{c,j}$ guarantee that we can apply the Laplace transform to (39) (see details
 471 in SM1.3). We obtain:

(49)

$$\int_0^\infty M_{c+1,j}^a(t) e^{-\lambda_c t} dt = \prod_{k=c+1}^{j-1} \frac{2p_L^{(k)} d\mathcal{B}_k^*(\lambda_c)}{1 - 2p_S^{(k)} d\mathcal{B}_k^*(\lambda_c)} \times \frac{\int_0^a \hat{\rho}^{(j)}(s) ds}{(1 - 2p_S^{(j)} d\mathcal{B}_j^*(\lambda_c)) \times \hat{\rho}^{(j)}(0)}.$$

Combining (47), (48) and (49) and the value of $\hat{\rho}^{(j)}(0)$ given in (12), we obtain $\tilde{m}_j(a)$. \square

We also study the asymptotic behavior of the second moment in SM1.3 (see theorem SM1.8).

Remark 3.12. These results can be extended in a case when the mother cell is not necessary of age 0 (for the one layer case, see [2], p.153).

Remark 3.13. Using the same procedure as in theorem 3.11, we can obtain a better estimate for the convergence of the deterministic solution ρ than that in theorem 2.12. Indeed, we can consider the study of $h(t, x) = e^{-\lambda_{1,j} t} \rho(t, x) - \eta \hat{\rho}_{1,j}(x)$ where $\hat{\rho}_{1,j}$ is the eigenvector of the sub-system composed of the j -th first layer, and find the proper function $\phi_{1,j}$.

3.5. Numerical illustration. We perform a numerical illustration with age independent division rates (which satisfy hypothesis 2.2). Figure 3a illustrates the exponential growth of the number of cells, either for the original solution of the model (2) (left panel) or the renormalized solution (right panel), checking the results given in theorems 2.14 and SM1.8. Figure 3b instantiates the effect of the parameters b_1 and $p_S^{(1)}$ on the leading layer (left panel) and the asymptotic proportion of cells (right panel). Note that the layer with the highest number of cells is not necessary the leading one. As can be seen in Figure 4, the renormalized solutions of the SDE (2) and PDE (3) match the stable age distribution $\hat{\rho}$ (see theorems 2.11 and 2.14). Asymptotically, the age distribution decreases with age, which corresponds to a proliferating pool of young cells, and is consistent with the fact that $\hat{\rho}^{(j)}$ is proportional to $e^{-\lambda_c a} \mathbb{P}[\tau^{(j)} > a]$. The convergence speeds differ between layers (here, the leading layer is the first one and the stable state of each layer is reached sequentially), corroborating the inequality given in theorem 2.12.

4. Parameter calibration. Throughout this part, we will work under hypotheses 2.1, 2.15 and 2.16. As a consequence, the intrinsic growth rate per layer can be computed easily:

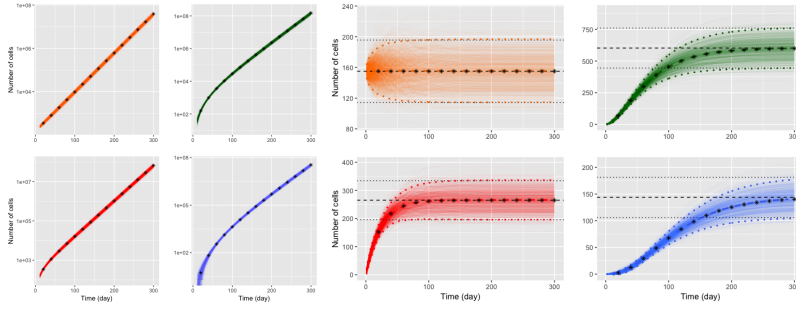
$$(50) \quad \lambda_j = (2p_S^{(j)} - 1)b_j \in] -b_j, b_j[, \text{ when } j < J.$$

4.1. Structural identifiability. We prove here the structural identifiability of our system following [8]. We start by a technical lemma.

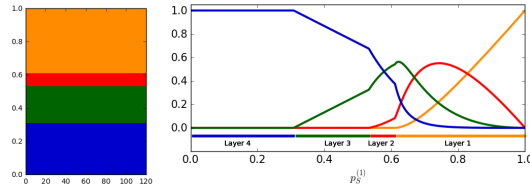
LEMMA 4.1. *Let M be the solution of (8). For any linear application $U : \mathbb{R}^J \rightarrow \mathbb{R}^J$, we have $[\forall t, M(t) \in \ker(U)] \Rightarrow [U = 0]$.*

Proof. *Ad absurdum*, if $U \neq 0$ and $M(t) \in \ker(U)$, for all t , then there exists a non-zero vector $u := (u_1, \dots, u_J)$ such that for all t , $u^T M(t) = 0$. This last relation, evaluated at $t = 0$ and thanks to the initial condition of (8), implies $u_1 = 0$. Then, derivating M , solution of (8), we obtain:

$$\frac{d}{dt} \sum_{j=2}^J u_j M^{(j)}(t) = 0 \Rightarrow \sum_{j=2}^J u_j [(b_{j-1} - \lambda_{j-1}) M^{(j-1)}(t) + \lambda_j M^{(j)}(t)] = 0.$$



(a) Exponential growth and asymptotic behavior



(b) Leading layer index and asymptotic proportion of cells

FIGURE 3. *Exponential growth and asymptotic moments.* **Figure 3a:** Outputs of 1000 simulations of the SDE (2) according to the algorithm SM1 with $p_S^{(j)}$, b_j given in Figure 1b, $p_{1,1}^{(j)} = 0$ and $Z_0 = 155\delta_{1,0}$. **Left panel:** the solid color lines correspond to the outputs of the stochastic simulations while the black stars correspond to the numerical solutions of the ODE (8) with the initial number of cells on the first layer $N = 155$ (orange: Layer 1, red: Layer 2, green: Layer 3, blue: Layer 4). **Right panel:** the color solid lines correspond to the renormalization of the outputs of the stochastic simulations by $e^{-\lambda c t}$. The black stars are the numerical solutions of the ODE (8). The color and black dashed lines correspond to the empirical means of the simulations and the analytical asymptotic means ($155\tilde{m}_j(\infty)$, theorem 2.14), respectively. The color and black dotted lines represent the empirical and analytical asymptotic 95% confidence intervals ($1.96\sqrt{v_j(\infty)}$, corollary SM1.10), respectively. **Figure 3b:** Leading layer index as a function of b_1 and $p_S^{(1)}$ (left panel) and proportion of cells per layer in asymptotic regime with respect to $p_S^{(1)}$ (right panel). In both panels, b satisfies (9) and $p_S^{(j)} = -15 * p_L^{(1)} * (j-1)^2 - 110 * p_L^{(1)} * (j-1) + p_S^{(1)}$.

511 Again, at $t = 0$, we obtain $u_2(b_1 - \lambda_1) = 0$. Because $\lambda_1 \neq b_1$, $u_2 = 0$. Iteratively,

$$512 \quad \forall j \in \llbracket 2, J \rrbracket, \quad u_j \prod_{k=1}^{j-1} (b_{k-1} - \lambda_{k-1}) = 0 \quad \Rightarrow \quad u_j = 0.$$

514 We obtain a contradiction. □

515 We can now prove theorem 2.17.

516 *Proof of theorem 2.17.* According to [8], the system (8) is \mathbf{P} -identifiable if, for
517 two sets of parameters \mathbf{P} and $\tilde{\mathbf{P}}$, $M(t; \mathbf{P}) = M(t; \tilde{\mathbf{P}})$ implies that $\mathbf{P} = \tilde{\mathbf{P}}$.

$$518 \quad \forall t \geq 0, M(t; \mathbf{P}) = M(t; \tilde{\mathbf{P}}) \Rightarrow \quad \frac{d}{dt} M(t; \mathbf{P}) = \frac{d}{dt} M(t; \tilde{\mathbf{P}})$$

$$519 \quad \Rightarrow \quad A_{\mathbf{P}} M(t; \mathbf{P}) = A_{\tilde{\mathbf{P}}} M(t; \tilde{\mathbf{P}}) = A_{\tilde{\mathbf{P}}} M(t; \mathbf{P})$$

$$520 \quad \Rightarrow \quad (A_{\mathbf{P}} - A_{\tilde{\mathbf{P}}}) M(t; \mathbf{P}) = 0$$

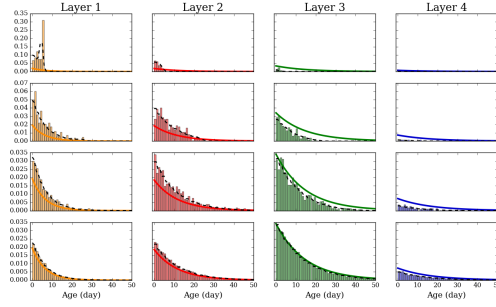


FIGURE 4. **Stable age distribution per layer.** Age distribution at different times of one simulation of the SDE (2) and of the PDE (3) using the algorithms described in respectively SM1 and SM2.0.2. We use the same parameters as in Figure 3. From top to bottom: $t = 5, 25, 50$ and 100 days. The color bars represent the normalized stochastic distributions. The black dashed lines correspond to the normalized PDE distributions, the color solid lines to the stable age distributions $\hat{\rho}^{(j)}$, $j \in \llbracket 1, 4 \rrbracket$. The details of the normalization of each lines are provided in SM2.1.

522 So, $M(t; \mathbf{P}) \in \ker(A_{\mathbf{P}} - A_{\tilde{\mathbf{P}}})$ and, from lemma 4.1, we deduce that $A_{\mathbf{P}} = A_{\tilde{\mathbf{P}}}$. Thus,

$$523 \begin{cases} (2p_S^{(j)} - 1)b_j = (2\tilde{p}_S^{(j)} - 1)\tilde{b}_j, & \forall j \in \llbracket 1, J \rrbracket, \\ 2p_L^{(j)}b_j = 2\tilde{p}_L^{(j)}\tilde{b}_j, & \forall j \in \llbracket 1, J-1 \rrbracket. \end{cases}$$

524 Using that $p_L^{(j)} = 1 - p_S^{(j)}$ and hypothesis 2.1, we deduce $\mathbf{P} = \tilde{\mathbf{P}}$. \square

525 **4.2. Biological application.** We now consider the application to the develop-
526 ment of ovarian follicles.

527 **4.2.1. Biological background.** The ovarian follicles are the basic anatomical
528 and functional units of the ovaries. Structurally, an ovarian follicle is composed of a
529 germ cell, named oocyte, surrounded by somatic cells (see Figure 5). In the first stages
530 of their development, ovarian follicles grow in a compact way, due to the proliferation
531 of somatic cells and their organization into successive concentric layers starting from
one layer at growth initiation up to four layers.

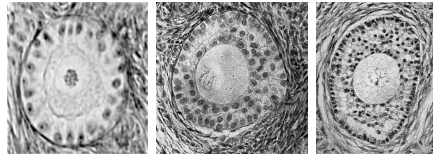


FIGURE 5. **Histological sections of ovarian follicles in the compact growth phase.** Left panel: one-layer follicle, center panel: three-layer follicle, right panel: four-layer follicle. Courtesy of Danielle Monniaux.

532

533 **4.2.2. Dataset description.** We dispose of a dataset providing us with mor-
534 phological information at different development stages (oocyte and follicle diameter,
535 total number of cells), and acquired from *ex vivo* measurements in sheep fetus [5]. In
536 addition, from [14, 13], we can infer the transit times between these stages: it takes
537 15 days to go from one to three layers and 10 days from three to four layers. Hence
538 (see Table 1a), the dataset consists of the total numbers of somatic cells at three time
539 points.

	$t = 0$	$t = 20$	$t = 35$
Data points (62)	34	10	18
Total cell number	113.89 \pm 57.76	885.75 \pm 380.89	2241.75 \pm 786.26
Oocyte diameter (μm)	49.31 \pm 8.15	75.94 \pm 10.89	88.08 \pm 7.43
Follicle diameter (μm)	71.68 \pm 13.36	141.59 \pm 17.11	195.36 \pm 23.95

(a) Summary of the dataset

Layer j	$p_S^{(j)}$	b_j	λ_j
1	0.6806	0.1146	0.0414
2	0.4837	0.0435	-0.0014
3	0.9025	0.0354	0.0285
4	1	0.0324	0.0324

(b) Estimated values of the parameters.

TABLE 1

Experimental dataset and estimated values of the parameters. Table 1b. The estimated value of α and the initial number of cells are respectively $\alpha = 1.633$ and $N \approx 155$. For $j \geq 2$, the b_j parameter values (in blue) were computed using formula (9). The λ_j values were computed using formula (50). The 95%-confidence intervals are $b_1 \in [0.0760; 0.1528]$, $\alpha \in [0.0231; 5.685]$, $N \in [126.4; 185.4]$, $p_S^{(1)} \in [0.6394; 0.7643]$, $p_S^{(2)} \in [0; 0.7914[$ and $p_S^{(3)} \in [0.6675; 0.9739]$.

We next take advantage of the spheroidal geometry and compact structure of ovarian follicles to obtain the number of somatic cells in each layer. Spherical cells are distributed around a spherical oocyte by filling identical width layers one after another, starting from the closest layer to the oocyte. Knowing the oocyte and somatic cell diameter (respectively d_O and d_s) and, the total number of cells N^{exp} , we compute the number of cells on the j th layer according to the ratio between its volume V^j and the volume of a somatic cell V^s :

$$\text{INITIALIZATION: } j \leftarrow 1, V^s \leftarrow \frac{\pi d_s^3}{6}, N \leftarrow N^{exp}$$

While $N > 0$:

$$V^j \leftarrow \frac{\pi}{6} [(d_O + 2 * j * d_s)^3 - (d_O + 2 * (j - 1) * d_s)^3]$$

$$N_j \leftarrow \min\left(\frac{V^j}{V^s}, N\right), N \leftarrow N - N_j, j \leftarrow j + 1$$

$$J \leftarrow j - 1$$

The corresponding dataset is shown on the four panels of Figure 2.

4.2.3. Parameter estimation. Before performing parameter estimation, we take into account additional biological specifications on the division rates. The oocyte produces growth factors whose diffusion leads to a decreasing gradient of proliferating chemical signals along the concentric layers, which results to the recurrence law (9) similar as that initially proposed in [1]. Considering a regression model with an additive gaussian noise, we estimate the model parameters to fit the changes in cell numbers in each layer (see SM2.2 for details). The estimated parameters are provided in Table 1b and the fitting curves are shown in Figure 2. We compute the profil likelihood estimates [11] and observe that all parameters are practically identifiable except $p_S^{(2)}$ (Figure SM1a). In contrast, when we perform the same estimation procedure on the total cell numbers, most of the parameters are not practicality identifiable (dataset in Table 1a, see detailed explanations in SM2.2).

5. Conclusion. In this work, we have analyzed a multi-type age-dependent model for cell populations subject to unidirectional motion, in both a stochastic and deterministic framework. Despite the non-applicability of either the Perron-Frobenius or Krein-Rutman theorem, we have taken advantage of the asymmetric transitions between different types to characterize long time behavior as an exponential Malthus growth, and obtain explicit analytical formulas for the asymptotic cell number moments and stable age distribution. We have illustrated our results numerically, and

572 studied the influence of the parameters on the asymptotic proportion of cells, Malthus
 573 parameter and stable age distribution. We have applied our results to a morphody-
 574 namic process occurring during the development of ovarian follicles. The fitting of the
 575 model outputs to biological experimental data has enabled us to represent the com-
 576 pact phase of follicle growth. Thanks to the flexibility allowed by the expression of
 577 morphodynamic laws in the model, we intend to consider other non-compact growth
 578 stages.

579 **6. Acknowledgments.** We thank Ken McNatty for sharing for the experimen-
 580 tal dataset and Danielle Monniaux for helpful discussions.

581

REFERENCES

- 582 [1] F. CLÉMENT, P. MICHEL, D. MONNIAUX, AND T. STIEHL, Coupled Somatic Cell Kinetics and
 583 Germ Cell Growth: Multiscale Model-Based Insight on Ovarian Follicular Development,
 584 Multiscale Model. Simul., 11 (2013), pp. 719–746, <https://doi.org/10.1137/120897249>.
 585 [2] T. E. HARRIS, The theory of branching processes, Springer-Verlag, 1963.
 586 [3] P. JAGERS AND F. C. KLEBANER, Population-size-dependent and age-dependent branching
 587 processes, Stochastic Process. Appl., 87 (2000), pp. 235–254, [https://doi.org/10.1016/](https://doi.org/10.1016/S0304-4149(99)00111-8)
 588 [S0304-4149\(99\)00111-8](https://doi.org/10.1016/S0304-4149(99)00111-8).
 589 [4] F. C. KLEBANER, Introduction to stochastic calculus with applications, Imperial College Press,
 590 3 ed., 2012.
 591 [5] T. LUNDY, P. SMITH, A. O’CONNELL, N. L. HUDSON, AND K. P. MCNATTY, Populations of
 592 granulosa cells in small follicles of the sheep ovary, J. Reprod. Fertil., 115 (1999), pp. 251–
 593 262.
 594 [6] J. A. METZ AND O. DIEKMANN, The dynamics of physiologically structured populations, vol. 68,
 595 Springer-Verlag, 1986.
 596 [7] P. MICHEL, S. MISCHLER, AND B. PERTHAME, General relative entropy inequality: an
 597 illustration on growth models, J. Math. Pures Appl. (9), 84 (2005), pp. 1235–1260,
 598 <https://doi.org/10.1016/j.matpur.2005.04.001>.
 599 [8] A. PERASSO AND U. RAZAFISON, Identifiability problem for recovering the mortality rate in an
 600 age-structured population dynamics model, Inverse Probl. Sci. Eng., 24 (2016), pp. 711–
 601 728, <https://doi.org/10.1080/17415977.2015.1061522>.
 602 [9] B. PERTHAME, Transport Equations in Biology, Birkhäuser Verlag, 2007.
 603 [10] P. E. PROTTER, Stochastic Integration and Differential Equations, Springer, 2nd ed., 2004.
 604 [11] A. RAUE, C. KREUTZ, T. MAIWALD, J. BACHMANN, M. SCHILLING, U. KLINGMÜLLER, AND
 605 J. TIMMER, Structural and practical identifiability analysis of partially observed dynamical
 606 models by exploiting the profile likelihood, Bioinformatics, 25 (2009), pp. 1923–1929, <https://doi.org/10.1093/bioinformatics/btp358>.
 607 [12] A. RAUE, B. STEIERT, M. SCHELKER, C. KREUTZ, T. MAIWALD, H. HASS, J. VANLIER,
 608 C. TÖNSING, L. ADLUNG, R. ENGESSER, W. MADER, T. HEINEMANN, J. HASENAUER,
 609 M. SCHILLING, T. HÖFER, E. KLIPP, F. THEIS, U. KLINGMÜLLER, B. SCHÖBERL, AND
 610 J. TIMMER, Data2dynamics: a modeling environment tailored to parameter estimation
 611 in dynamical systems, Bioinformatics, 31 (2015), pp. 3558–3560, [https://doi.org/10.1093/](https://doi.org/10.1093/bioinformatics/btv405)
 612 [bioinformatics/btv405](https://doi.org/10.1093/bioinformatics/btv405).
 613 [13] P. SMITH, R. BRAW-TAL, K. CORRIGAN, N. L. HUDSON, D. A. HEATH, AND K. P. MCNATTY,
 614 Ontogeny of ovarian follicle development in Booroola sheep fetuses that are homozygous
 615 carriers or non-carriers of the FecB gene, J Reprod Fertil, 100 (1994), pp. 485–490, <https://doi.org/10.1530/jrf.0.1000485>.
 616 [14] P. SMITH, W.-S. O, N. L. HUDSON, L. SHAW, D. A. HEATH, L. CONDELL, D. J. PHILLIPS, AND
 617 K. P. MCNATTY, Effects of the Booroola gene (FecB) on body weight, ovarian development
 618 and hormone concentrations during fetal life, J Reprod Fertil, 98 (1993), pp. 41–54, <https://doi.org/10.1530/jrf.0.0980041>.
 619 [15] V. C. TRAN, Large population limit and time behaviour of a stochastic particle model describing
 620 an age-structured population, ESAIM Probab. Stat., 12 (2008), pp. 345–386, <https://doi.org/10.1051/ps:2007052>.
 621 [16] G. F. WEBB, Theory of nonlinear age-dependent population dynamics, CRC Press, 1985.

Comment citer ce document :

Yvinec, R., Clément, F., Robin, F. (2017). Analysis and calibration of a linear model for structured cell populations with an application to the oogenesis of ovarian follicles. arxiv preprint, arXiv:1712.05372, 1-21.